

## The first giant flare from SGR 1806–20: observations with the INTEGRAL SPI Anti-Coincidence Shield

S. Mereghetti<sup>1</sup>, D. Götz<sup>1</sup>, A. von Kienlin<sup>2</sup>, A. Rau<sup>2</sup>, G. Lichti<sup>2</sup>, G. Weidenspointner<sup>3</sup>, P. Jean<sup>3</sup>

### ABSTRACT

A giant flare from the Soft Gamma-ray Repeater SGR 1806–20 has been discovered with the INTEGRAL gamma-ray observatory on 2004 December 27 and detected by many other satellites. This tremendous outburst, the first one observed from this source, was a hundred times more powerful than the two giant flares previously observed from other Soft Gamma-ray Repeaters (SGR). The 50 ms resolution light curve obtained with the Anticoincidence Shield of the INTEGRAL spectrometer SPI, which provides a high effective area above  $\gtrsim 80$  keV, shows evidence for emission lasting about one hour after the start of the outburst. This component, which decays in time as  $\sim t^{-0.85}$ , could be the first detection of a hard X-ray afterglow associated to an SGR giant flare. The short (0.2 s) initial pulse was so strong to saturate the detector for  $\sim 0.7$  s, and its backscattered radiation from the Moon was detected 2.8 s later. The following  $\sim 400$  s long tail, modulated at the neutron star rotation period of 7.56 s, had a fluence of  $2.6 \times 10^{-4}$  erg  $\text{cm}^{-2}$  above 80 keV, which extrapolating to lower energies corresponds to an emitted energy of  $1.6 \times 10^{44} d_{15kpc}^2$  erg at  $E > 3$  keV. This is of the same order of that in the pulsating tails of the two giant flares seen from other SGRs, despite the hundredfold larger overall emitted energy of the 2004 December 27 event.

*Subject headings:* stars: individual (SGR 1806–20) – stars: neutron – X-rays: bursts – Gamma-rays: bursts

---

<sup>1</sup>Istituto di Astrofisica Spaziale e Fisica Cosmica, Sezione di Milano "G.Occhialini" - INAF v.Bassini 15, I-20133 Milano, Italy

<sup>2</sup>Max-Planck-Institut für extraterrestrische Physik, Giessenbachstrasse, Postfach 1312, D-85741 Garching, Germany

<sup>3</sup>Centre d'Étude Spatiale des Rayonnements, 31028 Toulouse, France

## 1. Introduction

Soft Gamma-ray Repeaters (SGRs) are high-energy sources characterized by sporadic periods of activity in which they emit short bursts ( $<1$  s) with energy up to  $\sim 10^{41}$  erg. They are believed to be highly magnetized ( $B \sim 10^{14} - 10^{15}$  G) neutron stars, or "magnetars" (see Woods & Thompson 2004 for a recent review). Large soft  $\gamma$ -ray flares, reaching peak luminosities above several  $10^{44}$  erg  $s^{-1}$  and lasting a few minutes, have been observed from two SGRs: on 1979 March 5 from SGR 0525–66 (Mazets et al. 1979) and on 1998 August 27 from SGR 1900+14 (Hurley et al. 1999; Feroci et al. 1999). The detection of only two of such giant flares from different sources in about 30 years implies that these events, involving energy releases of more than  $10^{44}$  ergs, are relatively rare.

SGR 1806–20 is currently the most prolific of the four known SGRs. Its level of activity has been increasing in the last few years, during which many bursts have been detected with different satellites, including RXTE (Gögüş et al. 2001; Ibrahim et al. 2003; Woods et al. 2004) and INTEGRAL (Götz et al. 2004). On 2004 October 5 two clusters of strong bursts with a total fluence of  $\sim 10^{-4}$  erg  $cm^{-2}$  were emitted within a time span of a few minutes (Mereghetti et al. 2004). It was noted (Golenetskii et al. 2004) that a similar event occurred in SGR 1900+14 three months before its 1998 giant flare (Aptekar et al. 2001). The increasing level of activity in SGR 1806–20 was also reflected in the properties of its quiescent X-ray emission. XMM-Newton observations showed that its 2-10 keV luminosity doubled and the spectrum became harder in 2004 (Mereghetti et al. 2005b). A similar trend was present in the persistent 20-150 keV emission discovered with INTEGRAL observations carried out in 2003-2004 (Mereghetti et al. 2005a).

The energetic activity of SGR 1806–20 culminated on 2004 December 27, when the INTEGRAL satellite discovered the first giant outburst from this source (Borkowski et al. 2004). More than twenty satellites recorded this exceptional event which started with a hard pulse so intense to saturate most detectors (Hurley et al. 2005; Mazets et al. 2005; Palmer et al. 2005; Terasawa et al. 2005) and to significantly ionize the Earth's upper atmosphere (Campbell et al. 2005). Here we report the properties of this giant outburst derived with the Anti-Coincidence Shield (ACS) of the Spectrometer on board INTEGRAL (SPI, Vedrenne et al. 2003).

## 2. The Anti-Coincidence Shield of SPI

The ACS consists of 91 bismuth germanate (BGO) scintillator crystals of thickness between 16 and 50 mm and with a total mass of 512 kg. Besides serving as a veto for

the SPI germanium spectrometer, the ACS is able to detect gamma-ray bursts from a large fraction of the sky (von Kienlin et al. 2003). The data used here consist of the overall ACS count rate (i.e. the read out from the sum of the 91 crystals) sampled in time intervals of 50 ms. No energy or directional information is available. The ACS is sensitive to photons above a low-energy threshold corresponding to approximately 80 keV. However, due to the different properties of the various BGO blocks, their associated photomultipliers, and the chosen redundancy concept (the signals from two different crystals are fed to the same front-end electronics), this threshold is not sharp and its exact value not well determined.

Dead time and saturation effects in the crystals and electronics are negligible ( $<1\%$ ) for total count rates smaller than a few  $10^5$  cts  $s^{-1}$ . When this condition is verified we can easily convert the observed count rates to an incident energy flux, assuming a spectral shape and knowing the ACS effective area. The latter is a function of the incidence angle, with a maximum for directions nearly orthogonal to the satellite pointing axis and unobstructed by other instruments. At the time of the flare SGR 1806–20 was at a zenith angle  $\theta=106^\circ$  from the SPI pointing axis and at an azimuth angle  $\phi=9^\circ$  ( $\phi=0^\circ$  corresponds to the satellite Sun-pointing side, i.e. the direction from SPI toward the IBIS instrument). The ACS effective area as a function of energy for this direction has been computed by means of Monte Carlo simulations based on detailed mass modelling (Weidenspointner et al. 2003, and references therein) of SPI and of the surrounding material (satellite structure and other instruments). The effective area increases monotonically with energy; it is  $\sim 340$   $\text{cm}^2$  at 100 keV,  $\sim 1150$   $\text{cm}^2$  at 200 keV, and larger than  $3000$   $\text{cm}^2$  above 1 MeV. Thus the ACS provides the data with the best statistics in the soft  $\gamma$ -ray range available for this giant flare. For an optically thin thermal bremsstrahlung spectrum with  $kT_{br}=30$  keV we obtain a conversion factor of 1 ACS count  $s^{-1} \sim 4.3 \times 10^{-10}$   $\text{erg cm}^{-2} s^{-1}$  (80-2000 keV).

### 3. Properties of the giant flare

The total light curve of the flare, obtained by binning at 2.5 s the original ACS data, is shown in Fig. 1, while Fig. 2 displays at full resolution (50 ms) the initial part of the pulsating tail. We have defined  $t=0$  at 21:30:26.55 UT of 2004 December 27, approximately coinciding with the rise time of the flare. The giant flare starts with a short and extremely intense spike<sup>4</sup>. The measured count rate at the peak,  $\sim 2 \times 10^6$  counts  $s^{-1}$ , is strongly affected by dead time and saturation effects which cannot be easily modelled and prevent reliable flux estimates. A fit with a constant to the count rate in a 2 ks long time interval

---

<sup>4</sup>the Y-axis scale in Fig. 1 is cut at  $1.05 \times 10^5$  counts  $s^{-1}$  to better show the flare tail

before the flare yields a count rate of  $\sim 8.8 \times 10^4$  counts  $s^{-1}$ , which we use in the following analysis as a constant background level and include in all the fits keeping its value fixed.

A narrow burst, lasting  $\sim 0.2$  s, occurs at  $t=2.8$  s (see Fig. 2). Since this delay corresponds to the time taken by the wavefront to travel from INTEGRAL to the Moon and back to the satellite, this burst can be explained as backscattered radiation of the initial spike. A similar detection was reported with the Helicon-Coronas-F satellite, which could not observe directly SGR 1806–20 due to Earth occultation (Mazets et al. 2005). Assuming for the backscattered radiation the spectral shape derived by the above authors ( $dN/dE \propto E^{-0.7} \exp(-E/800 \text{ keV})$ ), we obtain a fluence of  $\sim 2 \times 10^{-6}$  erg  $cm^{-2}$  ( $E > 80$  keV). The duration and the fluence of the backscattered radiation are consistent with the properties of the initial spike (Mazets et al. 2005; Hurley et al. 2005; Terasawa et al. 2005).

The inset of Fig. 1 shows the light curve of the precursor burst which occurred 143 s before the flare. Triangulation analysis, using the ACS light curve together with data from other satellites, demonstrates that its arrival direction is consistent with the position of SGR 1806–20 (Hurley et al. 2005). The above authors, using the RHESSI satellite, found that the precursor spectrum can be crudely approximated by a thermal bremsstrahlung with  $kT_{br}=15$  keV and reported a fluence of  $1.8 \times 10^{-4}$  erg  $cm^{-2}$  for  $E > 3$  keV. Assuming the same spectrum, we obtain a fluence above 80 keV of  $4.4 \times 10^{-6}$  erg  $cm^{-2}$ , which extrapolated to lower energy overestimates the RHESSI value by a factor ten. Considering the uncertainties in the instruments cross calibration and the extrapolation largely dependent on the poorly determined spectrum, we do not consider this discrepancy as particularly significant. For instance, for  $kT_{br}=30$  keV we get  $F(>80 \text{ keV})=4.0 \times 10^{-6}$  erg  $cm^{-2}$  and  $F(>3 \text{ keV})=10^{-4}$  erg  $cm^{-2}$ . The phase of the event rise time with respect to the 7.56 s pulsations<sup>5</sup> is  $\phi \sim 0.1$ , which does not correspond to any of the peaks seen in the pulsating tail.

The transition from the initial spike to the pulsating tail is well fitted, in the time interval 1.2–2.2 s, by a power law function  $F \propto t^{-\delta}$  with  $\delta=2.1 \pm 0.1$  (Fig. 2). The broad bump in the time range  $\sim 2$ –5 s, as well as the following ones after  $t=10$  s, are in phase with the main peak of the 7.56 s pulsations ( $\phi=0.35$ –0.6) and can therefore be considered as the first appearance of the periodicity. The average profile of the pulsations is shown in Fig. 3 for different time intervals. An evolution of the profile during the flare, with the relative intensity of the peak at  $\phi=0.75$  increasing with time, is evident.

To characterize the long-term decay profile removing the effect of the pulsations, we binned the data in time intervals of 7.56 s. The resulting light curve (inset of Fig. 2) is well fit-

---

<sup>5</sup>since our data allow to determine the pulsation period with an accuracy of only  $\sim 0.1$  s, we adopt the more precise value obtained with RXTE (Woods et al. 2005) and define phase  $\phi=0$  at  $t=0$  s

ted in the time interval  $t \sim 15\text{--}400$  s by an exponential function with decay constant  $\tau = 138 \pm 5$  s. Note that the first bin ( $t = 7.56\text{--}16.2$  s) does not contain the initial hard spike. Nevertheless it lies significantly above the fitted function. Assuming a thermal bremsstrahlung spectrum with  $kT_{br} = 30$  keV, similar to the giant flares tails of other SGRs, the fluence in the time interval 1–400 s is  $\sim 2.6 \times 10^{-4}$  erg  $\text{cm}^{-2}$  for  $E > 80$  keV. Extrapolating the same spectral shape to lower energy, this corresponds to  $F(>3 \text{ keV}) \sim 6.4 \times 10^{-3}$  erg  $\text{cm}^{-2}$ .

#### 4. Afterglow emission

Our data show evidence for a second, separate component in addition to the main flare discussed above. After the end of the pulsating tail, at  $t \sim 400$  s, the count rate increases again, forming a long bump which peaks around  $t \sim 600\text{--}800$  s and returns to the pre-flare background level at  $t \sim 3000\text{--}4000$  s (see Fig. 4).

The ACS count rate is dominated by the incident flux of charged particles which varies on different time scales, due to the satellite motion and to the temporal and spatial variations in the flux of cosmic rays and trapped radiation. A long term ACS light curve covering almost one day and including the SGR 1806–20 giant flare is shown in the top panel of Fig. 5. For comparison, the lower panel of Fig. 5 shows the light curve obtained in the same time interval with the Plastic Scintillator Anti-Coincidence (PSAC), a thin (5 mm) detector located just below the SPI coded mask aperture, which is sensitive to charged particles and almost completely transparent to hard X-ray photons. It can be noted that both the long term trend and most of the fluctuations on shorter time scales are present in both detectors, as expected for charged particle induced background. On the contrary, the bump at  $t = 400\text{--}4000$  s is prominent only in the ACS, indicating its hard X-rays nature. Known variable sources, like e.g. Cyg X–1, are not bright enough in the hard X-rays to produce the count rate excess seen in the ACS, and no new transients were reported at the time of this observation. We also checked that the Sun was not particularly active in X-rays, by looking at the publicly available data of the GOES satellites<sup>6</sup>. We therefore conclude that the re-brightening after  $t = 400$  s and lasting about one hour is associated with SGR 1806–20. To our knowledge, this component has not been reported using data from other satellites. This might be due to background variability and source occultation effects in low Earth orbit satellites and to the lack of sufficient sensitivity at hard X-rays in other detectors.

After accounting for the background, estimated from a linear fit to the ACS count rate for  $t < 0$  s and  $t > 4000$  s, the time profile decay in the interval  $t = 500\text{--}4000$  s can be reasonably

---

<sup>6</sup><http://www.sec.noaa.gov/>

well described as a power law  $F \propto t^{-\delta}$  with  $\delta \sim 0.85$ . The fluence in the 400–4000 s time interval is approximately equal to that contained in the pulsating tail ( $t=1\text{--}400$  s).

## 5. Discussion

The most striking difference between the 2004 December 27 outburst of SGR 1806–20 and the giant flares previously observed from SGR 0526–66 and SGR 1900+14 is the global energetics of the event. For a distance of 15 kpc (Corbel & Eikenberry 2004), the hard X–ray fluence in the SGR 1806–20 initial spike (Hurley et al. 2005; Terasawa et al. 2005) implies an isotropic-equivalent energy release of several  $10^{46}$   $d_{15}^2$  erg. This is at least two orders of magnitude larger than that of the two other giant flares ( $1.6 \times 10^{44}$  erg for SGR 0526–26;  $> 7 \times 10^{43}$  erg for SGR 1900+14). The much higher involved energy is also reflected in the properties of the transient radio emission, which reached a luminosity a factor 500 (Cameron et al. 2005, Gaensler et al. 2005) larger than that seen in SGR 1900+14 after the 27 August 1998 event (Frail et al. 1999). On the other hand, the energy output in the SGR 1806–20 pulsating tail ( $1.6 \times 10^{44}$   $d_{15}^2$  erg for  $E > 3$  keV) is similar to that of SGR 1900+14 ( $5 \times 10^{43}$  erg) and of SGR 0526–66 ( $4 \times 10^{44}$  erg). The giant flare of SGR 1806–20 is thus characterized by a much higher spike-to-tail energy ratio ( $\gtrsim 100$ ) than the two previous events ( $\sim 1$ ). According to the magnetar model, essentially all the energy release occurs during the initial  $\sim 0.2$  s transient phase, when a hot relativistic fireball is launched. A fraction of this energy is trapped by closed field lines in the neutron star magnetosphere, forming an optically thick photon-pair plasma which evaporates giving rise to the radiation observed in the pulsating tail (Thompson & Duncan 1995). The magnetic field strength limits the amount of energy that can be confined. The fact that this quantity is similar in the three giant flares, despite the much higher total energy release of SGR 1806–20, is consistent with a magnetic field of the same order in the three magnetars.

The pulse profile and its time evolution observed with the ACS are similar to those seen with RHESSI and Swift (Hurley et al. 2005; Palmer et al. 2005), which are dominated by photons of lower energy. Thanks to the large effective area above 100 keV of the ACS, we can clearly see variations in the pulse profile at high energies. The different evolution of the emission components visible in the pulsating tail (see Fig. 3) suggests separate emission regions. It is interesting to note that the pulsations are present since the very early phase of the flare, as indicated by the broad pulse visible at  $t=2\text{--}5$  s (Fig. 2). This pulse persists at the same rotational phase in the following cycles, while a secondary peak at  $\phi \sim 0.75$  gradually emerges.

While the above results are similar to those obtained with other satellites, our data

provide unique evidence for a second, long lasting component in the hard X-ray light curve. The emission after  $t \sim 400$  s could originate from the neutron star surface and/or magnetosphere or, alternatively, from the interaction of the relativistic fireball with the surrounding medium. A search for pulsations in the ACS data after  $t = 400$  s gave a negative result, favoring the second interpretation. The afterglow produced by the SGR 1806–20 giant flare has been observed in the radio band (Gaensler et al. 2005; Cameron et al. 2005), yielding estimates of the minimum energy in magnetic field and relativistic particles,  $E$ , of several  $10^{43}$  erg (see also Nakar, Piran & Sari 2005). The hard X-ray fluence in the 400–3000 s time interval is consistent with this value. With simple gamma-ray burst afterglow models based on synchrotron emission we can estimate the bulk Lorentz factor  $\Gamma$  from the time  $t_0$  of the afterglow onset:  $\Gamma \sim 15 (E / 5 \cdot 10^{43} \text{ erg})^{1/8} (n / 0.1 \text{ cm}^{-3})^{-1/8} (t_0 / 100 \text{ s})^{-3/8}$ , where  $n$  is the ambient density (see, e.g. Zhang & Meszaros 2003, and references therein). This is smaller than the typical values for gamma-ray bursts, but consistent, considering the large involved uncertainties, with the mildly relativistic outflow inferred from the modelling of the radio data (Granot et al. 2005). Alternatively, the observed re-brightening could be due to an Inverse Compton component, implying a high density environment ( $n \gtrsim 10 \text{ cm}^{-3}$ ) and a high electron radiation efficiency.

We thank K. Hurley, G. Ghisellini, J. Borkowski and M. Feroci for useful comments. This work has been partially funded by the Italian Space Agency. The SPI-ACS is supported by the German "Ministerium für Bildung und Forschung" through the DLR grant 50.OG.9503.0.

## REFERENCES

- Aptekar R.L., Frederiks D.D., Golenetskii S.V. et al. 2001, ApJSS 137, 227  
Borkowski J., Götz D., Mereghetti S. et al. 2004, GCN Circ. n. 2920  
Cameron P.B. et al. 2005, submitted to Nature, astro-ph/0502428  
Campbell P. et al. 2005, GCN Circ. n. 2932  
Corbel S. & Eikenberry S.S. 2004, A&A 419, 191  
Feroci M. et al. 1999, ApJ 515, L9  
Frail D.A., Kulkarni, S.R. & Bloom, J.S., 1999, Nature, 398, 127  
Gaensler, B.M., et al., 2005, submitted to Nature, astro-ph/0502393  
Göğüş, E., Kouveliotou, C., Woods, P.M., et al. 2001, ApJ, 558, 228  
Golenetskii S.V., Aptekar R., Mazets E. et al. 2004, GCN Circular n. 2769

- Götz, D., Mereghetti S., Mirabel F.I. & Hurley K. 2004, A&A 417, L45
- Granot J., Ramirez-Ruiz E., Taylor G.B. et al. 2005, Submitted to ApJ, astro-ph/0503251
- Hurley K., Cline T., Mazets E. et al. 1999, Nature 397, 41
- Hurley K. et al. 2005, submitted to Nature, astro-ph/0502329
- Ibrahim A.I., Swank J.H. & Parke W. 2003, ApJ 584, L171
- Mazets E.P. et al. 1979, Nature 282, 587
- Mazets E.P. et al. 2005, astro-ph/0502541
- Mereghetti S., Götz D., Borkowski J. et al. 2004, GCN Circular n. 2763
- Mereghetti S., Götz D., Mirabel I.F & Hurley K. 2005a, A&A, in press, astro-ph/0411695
- Mereghetti S., Tiengo A., Esposito P. et al. 2005b, submitted to ApJ, astro-ph/0502417
- Nakar E., Piran T. & Sari R. 2005, astro-ph/0502052
- Palmer D. et al. 2005, submitted to Nature, astro-ph/0503030
- Terasawa, T. et al., 2005, submitted to Nature, astro-ph/0502315
- Thompson, C., & Duncan, R.C. 1995, MNRAS, 275, 255
- von Kienlin A., Beckmann V., Rau A., et al. 2003, A&A, 411, L299
- Vedrenne G., Roques J.-P., Schönfelder V., et al. 2003, A&A 411, L63
- Weidenspointner G., Kiener J., Gros M. et al. 2003, A&A 411, L113
- Woods P.M. & Thompson C. 2004, astro-ph/0406133
- Woods P.M., Kouveliotou C., Göğüş E., et al. 2004, The Astronomer's Telegram, 313
- Woods P.M., Finger M., Patel S. et al. 2005, GCN Circular n. 2950
- Zhang B. & Mészáros P. 2003, astro-ph/0311321



Fig. 1.— ACS light curve of the whole giant flare binned at 2.5 s. The peak of the flare, reaching an observed count rate  $\gtrsim 2 \times 10^6$  counts  $\text{s}^{-1}$ , is not shown. The inset shows the light curve of the precursor burst at full resolution (50 ms).

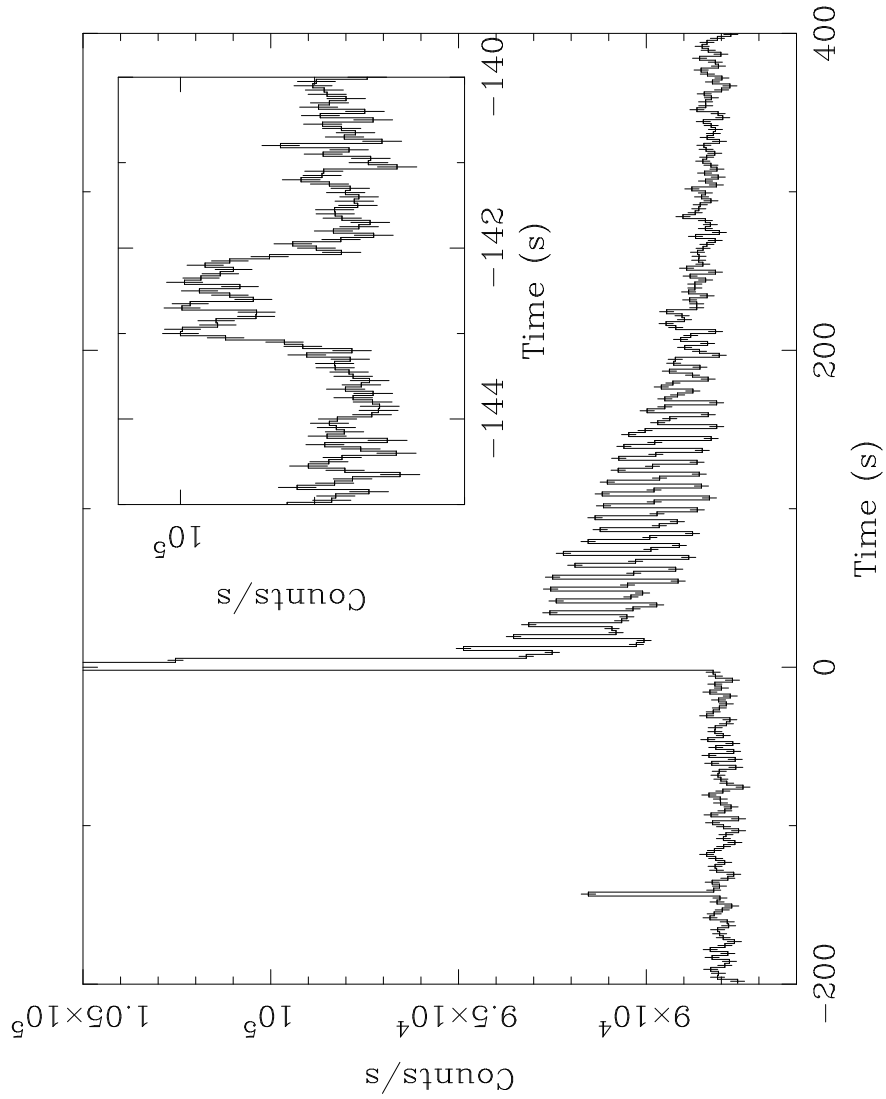


Fig. 2.— Declining part of the initial spike and initial part of the pulsating tail. The line is a fit with a power law plus a constant (fixed at the pre-flare level) to the count rate in the time interval 1.2–2.2 s. The narrow burst at  $t=2.8$  s is due to radiation from the initial spike backscattered by the Moon. The inset shows the light curve of the tail binned at the spin period (7.56 s) and fitted with an exponential function.

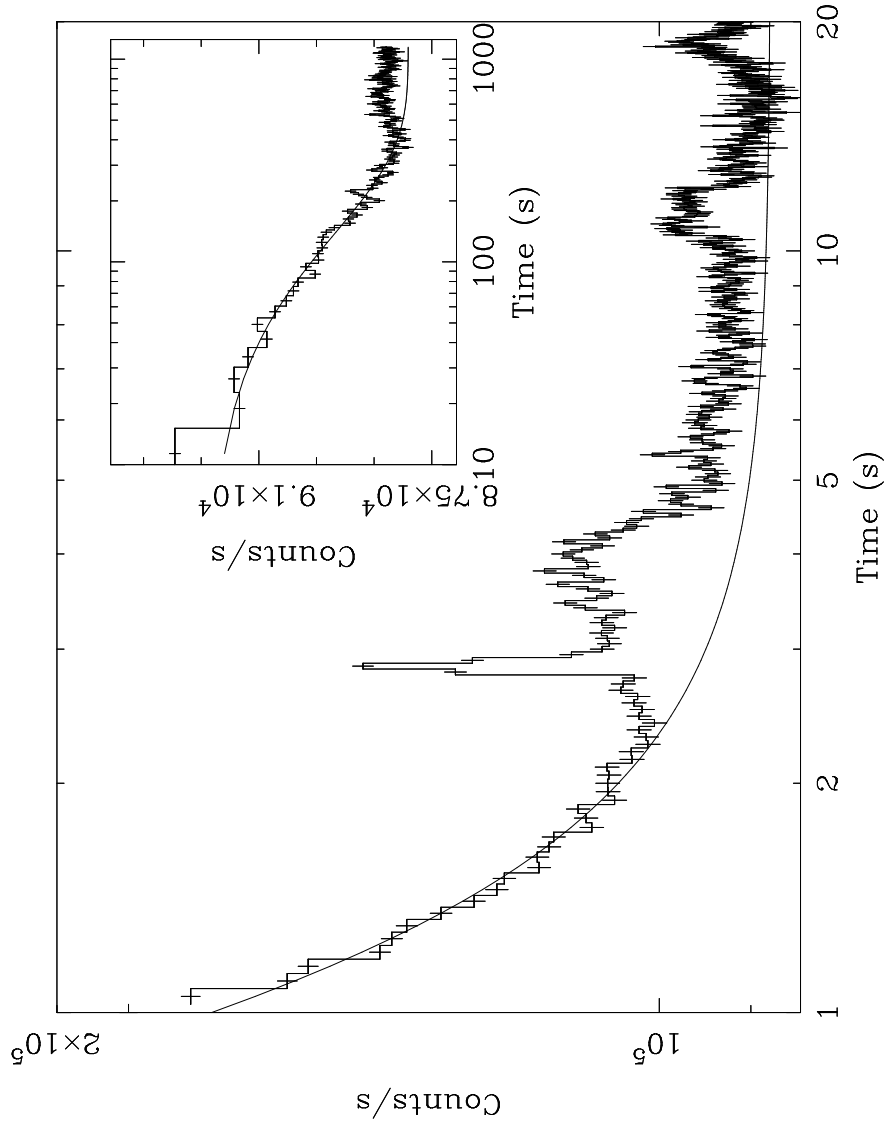


Fig. 3.— Averaged pulse profile obtained by folding the data in three time intervals at the spin period of 7.56 s.

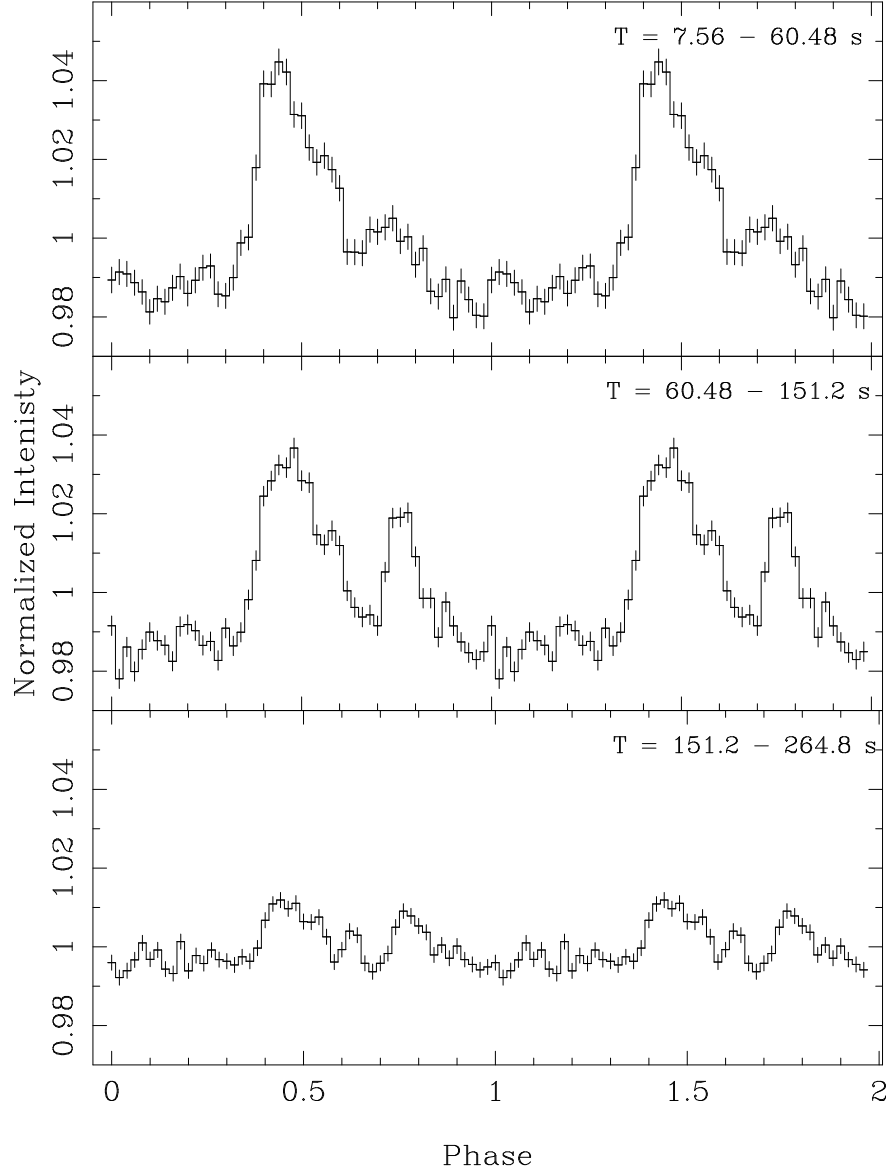


Fig. 4.— SPI ACS light curve of SGR 1806–20 binned at 50 s. The count rate settles back to the pre-flare level after  $t \sim 3000$ – $4000$  s.

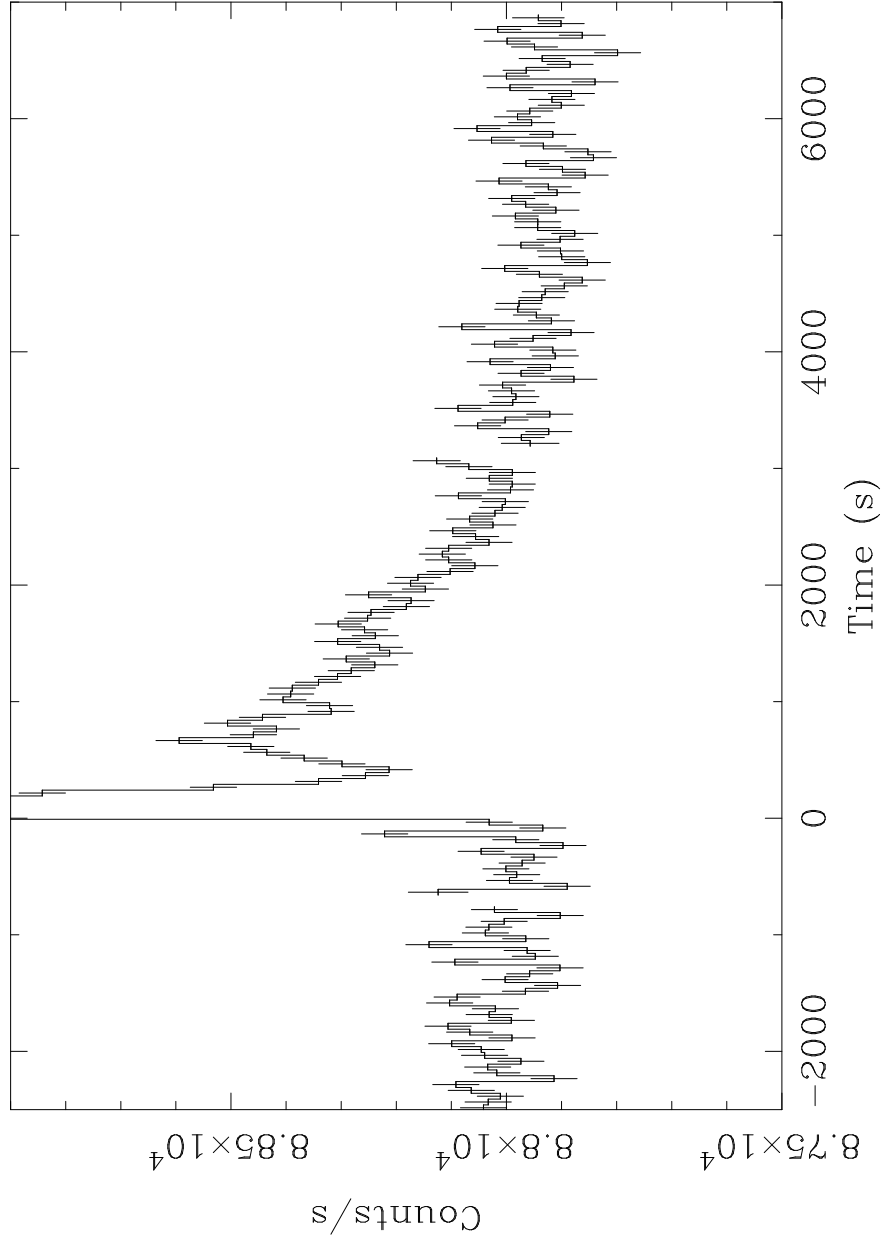


Fig. 5.— Comparison between the ACS (top) and PSAC (bottom) light curves. The long lasting emission after the giant flare is not visible in the PSAC, while particle induced variations are visible in both detectors (the narrow pulse at  $t \sim -10^4$  s in the ACS is a gamma-ray burst, unrelated to SGR 1806–20).

